Iranian Journal of Geophysics, Vol 15 No 4, 2022, Page 1 – 14 (Research Article)
DOI: 10.30499/IJG.2020.251600.1293

Impact of distribution of seismic ambient noise sources on surface wave characteristics

Naimeh Sadat Moghadasi[1] and Elham Shabani[2*]

[1] *Ph.D student, Department of Seismology, Institute of Geophysics, University of Tehran, Tehran, Iran*
[2] *Assistant Professor, Department of Seismology, Institute of Geophysics, University of Tehran, Tehran, Iran*

(Received: 19 December 2019, Accepted: 9 March 2020)

Abstract

The seismic ambient noise observation is widely used in site characterization studies to obtain the subsurface velocity structure because of the simplicity and low cost. Different single and array methods have been introduced in this field to study seismic ambient noise characteristics. In this paper, we investigated the effects of distributions of the seismic ambient noise sources on surface wave properties. In this regard, two datasets are simulated regarding omnidirectional and non-omnidirectional distributions of sources. In the former, it is assumed that the waves travel through the array from all even azimuths and for the latter, an arc shape distribution is considered. To process the data, the RTBF (Rayleigh three component beamforming) array signal processing technique is applied to retrieve Rayleigh and Love phase velocity dispersion curves and Rayleigh wave ellipticity. Furthermore, two well-known single station methods HVTFA (horizontal to vertical time frequency analysis) and RayDec (random decrement technique) are implemented to extract the ellipticity curves. For all the applied methods, impacts of the two considered distributions of sources are investigated. Then, the results are compared to theoretical curves which are computed from a specific earth model used to produce synthetic noise data. Moreover, a data recorded in Ramsar (north of Iran), as a typical case of non-omnidirectional distribution of noise sources, selected to justify our assertion in processing synthetic noise data. Benefitting the mentioned array and single station methods, the characteristics of surface waves are studied and the shear wave velocity profile is estimated by joint inversion of retrieved dispersion and ellipticity curves.

Keywords: Seismic noise, distribution of noise sources, ellipticity curve, dispersion curve, shear wave velocity profile, site effects

[*] Corresponding author: eshabani@ut.ac.ir

1 Introduction

In recent years, the analysis of seismic ambient noise has gained considerable attetion to obtain the subsurface shear wave velocity structure and to evaluate site effects (Bonnefoy-Claudet et al., 2006; Foti et al., 2011). A variety of array and single station methods is proposed to study different features of seismic ambient noise. Array-analysis-based methods are suitable to retrieve different aspects of surface waves such as dispersion and ellipticity curves. The most well-known array methods are as follows: The frequency-wavenumber (F-K) (Lacoss et al., 1969), the spatial autocorrelation (SPAC) (Aki, 1957; Köhler et al., 2007), the wavefield decomposition (WaveDec) (Maranò et al., 2012) and the high resolution Rayleigh three-component beamforming (RTBF) (Wathelet et al., 2018) methods.

The elliptical behavior of Rayleigh wave motion can be measured by both single station and array methods. The primary method to assess this aspect is the horizontal-to-vertical spectral ratio (H/V) (Nakamura, 1989; Nogoshi and Igarashi, 1971). This method is mainly used to determine the resonance frequency of the site. The main problem of retrieving ellipticity from this method is not to consider the energy of body and Love waves present in the seismic ambient noise recordings. In general, the seismic noise wavefield is composed of different modes of Rayleigh, Love and body waves and it is assumed that the wavefield is primarily dominated by surface wave (Fäh et al., 2001). The removal of Love wave's contribution in H/V calculation leads to a more accurate estimation of Rayleigh wave ellipticity. Different single station methods are proposed to suppress the effects of Love wave in retrieving ellipticity curve of Rayleigh waves, which the horizontal-to-vertical time frequency analysis (HVTFA) (Fäh et al., 2009) and RayDec (Hobiger et al. 2009) are the best candidates.

In this paper, to analyze the dependency of surface wave characteristics on the distribution of sources, two array datasets are simulated. The data was produced in an array of six stations for omnidirectional and non-omnidirectional noise source distributions. In the case of omnidirectional distribution, it is assumed that the sources are randomly distributed around the stations in evenly distributed azimuths. For non-omnidirectional noise distribution, the sources are randomly considered in azimuthal intervals. In order to investigate the impacts of different distributions of noise sources on surface wave characteristics, the RTBF is implemented to determine Rayleigh and Love phase velocity dispersion and ellipticity information. Moreover, HVTFA and RayDec methods are used to retrieve Rayleigh wave ellipticity curves on synthesized data. The obtained dispersion and ellipticity curves are compared to corresponding theoretical curves for each distribution. The theoretical curves obtained in the forward modeling from the known earth model are used to synthetize data. Furthermore, due to the presence of the Caspian Sea to the north of the array, real seismic noise measured in Ramsar, as a non-omnidirectional distribution case, is used to study surface wave characteristics. The ellipticity and dispersion curves of the fundamental mode of Rayleigh and Love waves are jointly inverted to obtain shear wave velocity of subsoil structure in the site.

2 Simulation of data

The synthetic seismic noise is simulated using FD code which was developed within the European SESAME project by Moczo and Kristek (2002). The steps are as follows: The ambient seismic noise sources are approximated by acting single forces that are randomly distributed in space, amplitude, direction and time. The surficial sources are randomly distributed

spatially from the surface to a depth of 0.5 m (Hobiger et al., 2009). The source time function is considered as delta-like signal and the wavefield is computed using the wavenumber method proposed by Hisada (1994, 1995). This method efficiently computes the Green's functions for viscoelastic horizontally stratified media with sources and stations located at equal or nearly depths (Hisada, 1995). Then, the response of the structure is convolved with the source time function. Finally, to obtain the synthetic noise data in the stations of the array, the synthetic time histories due to all source contributions are superposed.

In this study, an array including five three-component stations placed on the circumference of a circle and a central one with a radius of 100 m (Fig. 1a) and also a homogeneous layer over a half-space velocity model are considered to produce data (Table 1). Furthermore, two different distributions of sources around the stations are considered. First distribution which is called omnidirectional distribution, includes the sources contributed randomly around an array of stations so that the minimum and maximum distance between any source and station is 500 and 1500 m, respectively (Fig. 1b). Second distribution includes the sources located in an arc shaped distribution (in the southern part of the array) at a mean distance of 1000 m from the central station (Fig. 1c) in the case of non-omnidirectional distribution. Therefore, the waves with different azimuths travel through the array of stations for the first case, while for the second distribution, the received waves are from the same azimuthal intervals. 400 sources are used in this simulation. The length of the simulated signals is about 368 seconds with a sampling frequency of 80 Hz. Fig. 2 represents the velocity profile used to produce the data (according to Table 1) alongside the associated theoretical dispersion and ellipticity curves of fundamental and first higher modes of Rayleigh (R_0, R_1) and Love waves (L_0, L_1). The theoretical dispersion and ellipticity curves are computed from the known earth model in the forward computations using the Geopsy software (gpell and gpdc toolboxes) (Wathelet et al., 2020). Fig. 3 illustrates the vertical components simulated for simultaneous noise records in six stations of the array considering the two studied distributions.

Table 1. The earth model considered as a layer over half space applied to produce synthetic noise. D is the depth range. Vp and Vs are the pressure wave velocity and the shear wave velocity, respectively. ρ is the mean density. Q_p and Q_s are quality factors for P and S waves, respectively.

D (m)	V_p (m/s)	V_s (m/s)	ρ (kg/m^3)	Q_p	Q_s
35	500	200	1900	50	25
half space	2000	1000	2500	100	50

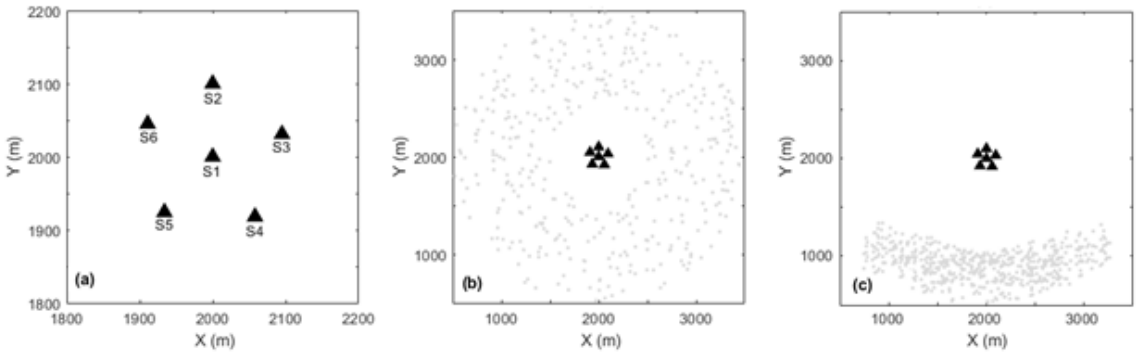

Fig 1. (a) The array layout composed of six stations with (b) the omnidirectional distribution of sources around the stations (full even azimuthal distribution) and (c) the non-omnidirectional (arc shaped) distributed sources. The stations and sources are depicted by black triangle and gray dots, respectively.

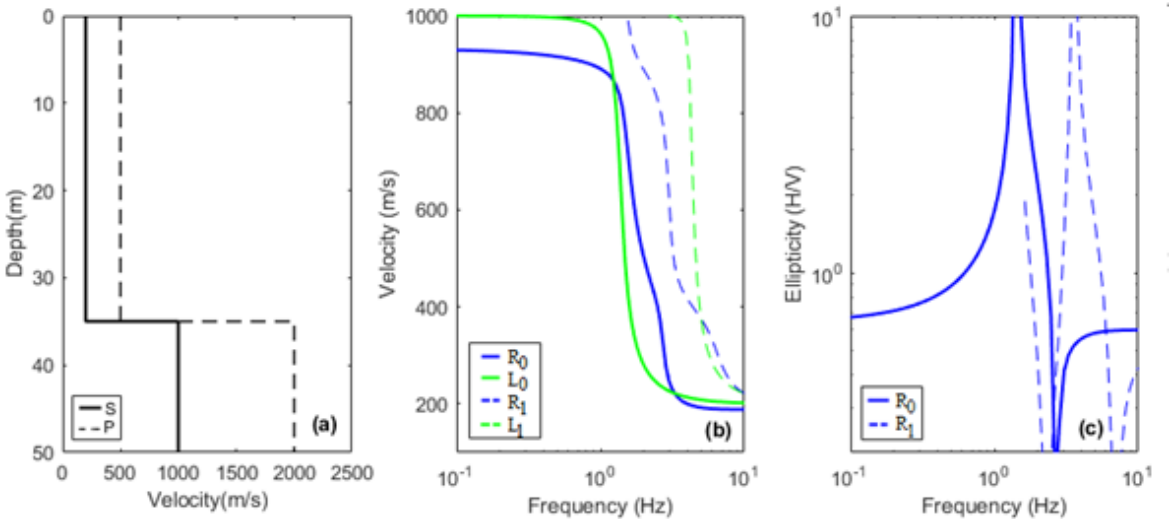

Fig 2. (a) The velocity profile of the underground (P and S waves) which is considered to produce synthetic noise data (b) the corresponding theoretical dispersion curves for R_0, R_1, L_0 and L_1 waves (c) the corresponding theoretical ellipticity curves of R_0 and R_1.

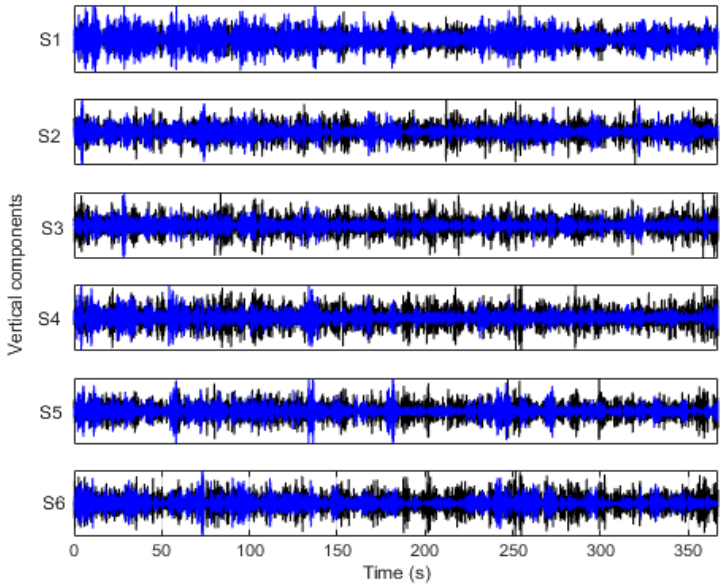

Fig 3. The simultaneous synthetic noise data on the vertical components at five stations placed on a circumference and one in the center for two distributions of sources, including omnidirectional and non-omnidirectional distributions shown by blue and black colors, respectively.

3 Methods and applications on the synthetic noise data

The synthetic seismic data are generally analyzed using both single station and array processing techniques. Single station methods identify properties of the subsurface underneath the station, such as the fundamental frequency of the site, while the array processing techniques make it possible to determine the velocity and azimuth of seismic waves crossing the array layout and also to identify Rayleigh and Love waves. In this study, the RTBF array methods alongside two single station methods HVTFA and RayDec are used to quantify the surface wave dispersion and ellipticity curves.

3-1 Rayleigh three-component beamforming (RTBF)

RTBF is a kind of high resolution frequency-wavenumber array processing technique which was proposed by Wathelet et al. (2018). The method developed to quantify ellipticity and phase-velocity dispersion using multicomponent beamforming. From the assumption that the seismic noise wavefield is dominated by surface waves, the properties of a beamforming is based on a compound cross spectral matrix which includes vertical and radial components. In fact, the cross spectral matrix is analogue to the time domain cross correlation which is used in signal processing to estimate the degree of correlation between signals. In analyzing noisy signal under the assumption of uncorrelation between signal and noise, the expected value of cross spectral matrix is defined as the product of Fourier transform of the signal and its conjugate transpose. In practice, the expected value is obtained from an average between several cross correlation snapshots of successive time windows (Poggi and Fäh, 2010).

In this method, the information of all components of the stations are combined into a single cross spectral matrix to obtain the dispersion curves of Rayleigh and Love waves and also the ellipticity angle of Rayleigh wave. Unlike the high resolution beamforming method (Capon, 1969) in which the cross spectral matrices have N×N elements (N is the number of three-component sensors), this method benefits using 2N×2N elements made of vertical and radial components. Combining the vertical and radial components in the computation of the cross-spectrum matrix improves the identification of higher modes of phase-velocity dispersion, especially at higher frequencies where the classical methods usually may fail (Wathelet et al., 2018). Furthermore, it is possible to extract the signed ellipticity information for three component stations directly from the maximization of the high resolution beam power (Wathelet et al., 2018). The ellipticity angle (signed ellipticity) is linked to the classical ellipticity as follows (Maranò et al., 2012):

$$\varepsilon = |\tan \xi| \quad (1)$$

where ε is the Rayleigh wave ellipticity and ξ indicates ellipticity angle. The ellipticity generally varies in the range of $[0, \infty)$, while the ellipticity angle is in the range of $[-\pi/2, \pi/2]$ which shows the sense of particle motion at any time (retrograde and prograde motions). For retrograde particle motion, the ellipticity angle has negative values $(-\pi/2, 0)$, while in the case of prograde motion, it varies in the range of 0 to $\pi/2$. Furthermore, the ellipticity angle reaches zero and $\pm\pi/2$ at trough and peak frequencies, respectively (Maranò et al., 2012). Fig. 4 represents the ellipticity and the ellipticity angle of the Rayleigh wave computed for the earth model in Table 1. The fundamental mode is retrograde at low frequencies, while the sense of motion changes to prograde at peak frequency (1.5 Hz) (Fig. 4b). The right flank of ellipticity in the frequency range of 1.5 to 2.7 Hz shows prograde particle motion, however, the sense of motion for higher frequencies changes to retrograde.

The RTBF technique is applied on the simulated data for two different distributions of noise sources (Fig. 5). It should be noted that the color scale in the background which describes the probability density of such estimates, is provided to improve the readability of the plot. The trends of highest probability densities are picked as mean values and the resultant curves are depicted in orange color with the relevant error bars representing standard deviations.

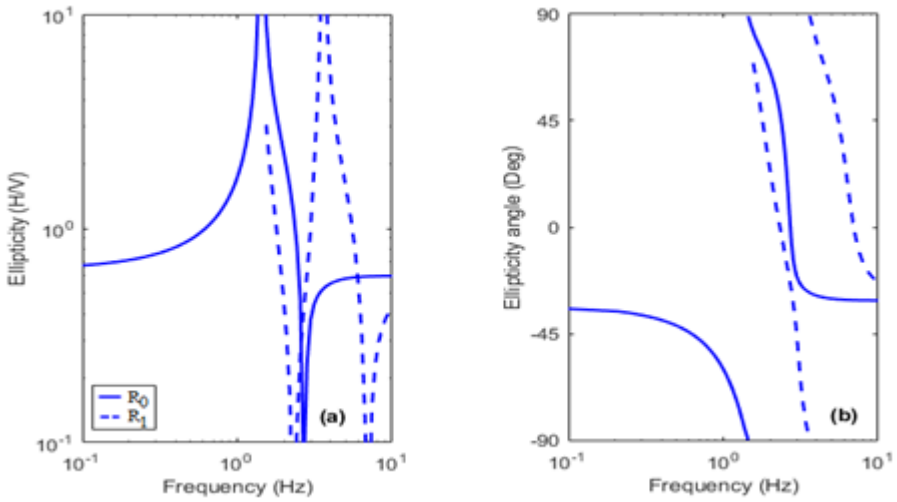

Fig 4. (a) The theoretical ellipticity curves (b) the ellipticity angles of the fundamental (R_0) and first higher mode (R_1) of Rayleigh wave based on the earth model in Table 1.

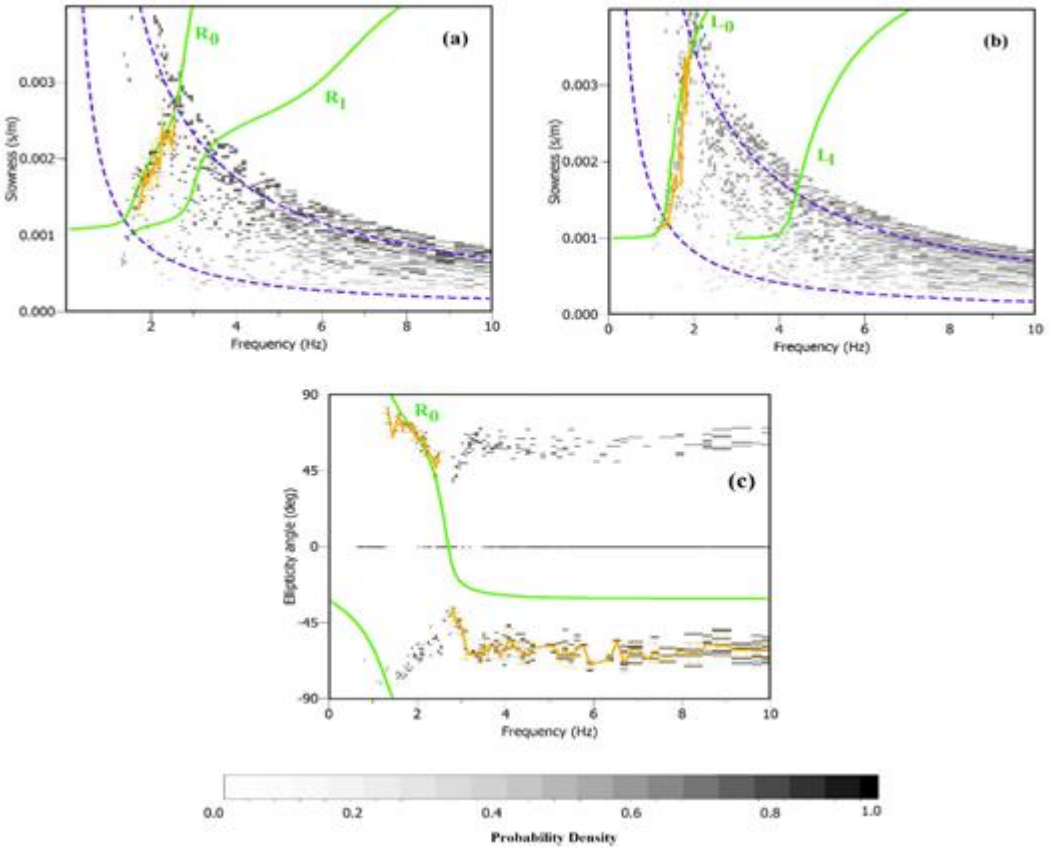

Fig 5. Applying RTBF method for synthetic data in omnidirectional distribution of noise sources (a) the estimated Rayleigh wave dispersion curves, the picked R_0 (in orange color) and theoretical R_0 and R_1 (the green curves) (b) the estimated Love wave dispersion curves, the picked L_0 (in orange color) and theoretical L_0 and L_1 (the green curves) (c) the estimated Rayleigh wave ellipticity angle, the picked R_0 (in orange color) and theoretical R_0 (the green curve). The array limits are shown by dashed blue curves. The color scale in the background is provided to improve the readability of the plot and describes the probability density of such estimates. The background is darker corresponding to many estimates with similar values and lighter when few estimates are present.

The resultant picked dispersion and ellipticity curves are compared to corresponding theoretical curves. As it is represented in Fig. 5a, the retrieved picked dispersion curves of R_0 and L_0 are in good agreement with the theoretical curves assuming the omnidirectional distribution of noise sources, however, dispersion curves of R_1 and L_1 are not recognizable (Figs. 5a and 5b). The picked ellipticity shows agreement to the theoretical model in a limited frequency range from 1.8 to 2.2 Hz where the motion is prograde (Fig. 5c). However, some discrepancies are seen for frequencies higher than 2.7 Hz.

In the case of non-omnidirectional distribution of noise sources, the picked R_0 and L_0 dispersion curves are in good agreement with corresponding theoretical model, and it seems that R_1 is recognizable (Figs. 6a and 6b). However, the recognition of the L_1 seems to be ambiguous. Ac

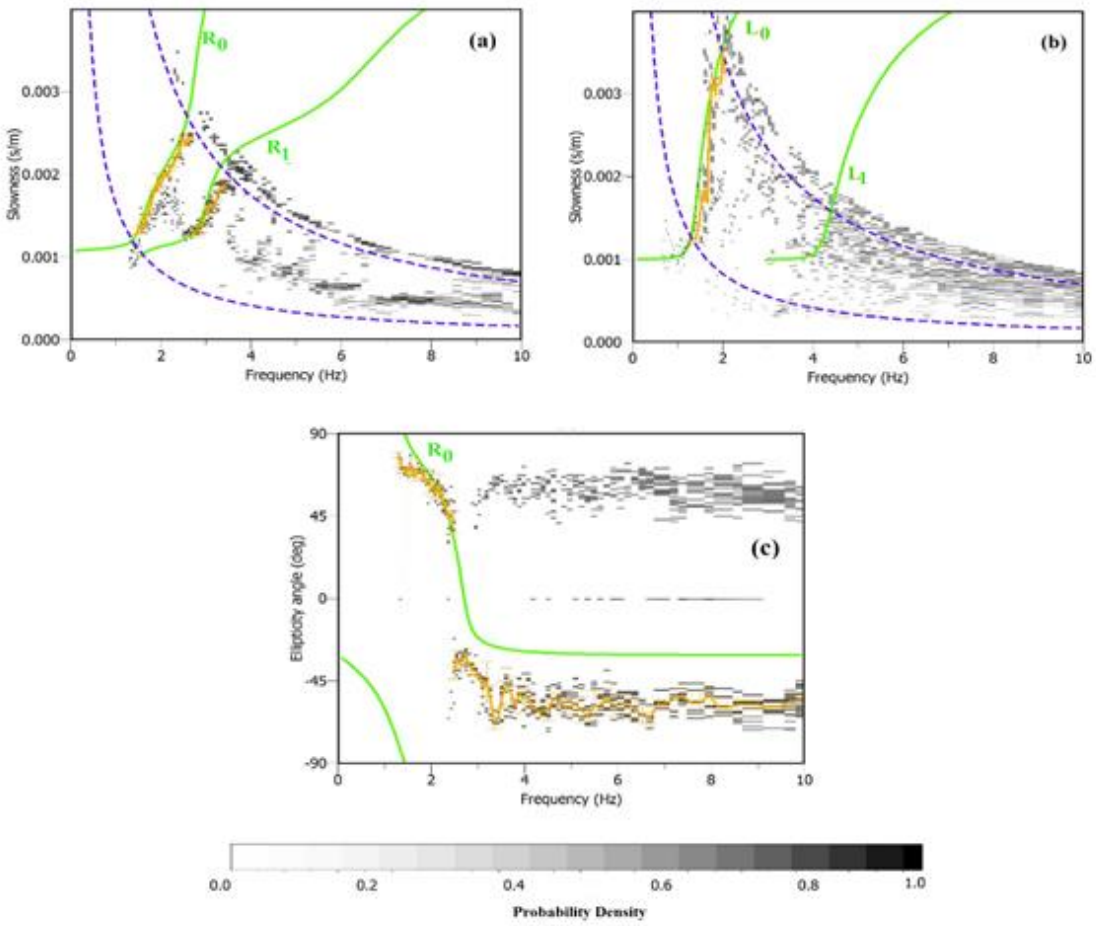

Fig 6. Applying RTBF method for synthetic data in non-omnidirectional distribution of noise sources (a) the estimated Rayleigh wave dispersion curves, the picked R_0 and R_1 (in orange color) and theoretical R_0 and R_1 (the green curves) (b) the estimated Love wave dispersion curves, the picked L_0 (in orange color) and theoretical L_0 and L_1 (the green curves) (c) the estimated Rayleigh wave ellipticity angle, the picked R_0 (in orange color) and theoretical R_0 (the green curve). The array limits are shown by dashed blue curves. The color scale in the background is provided to improve the readability of the plot and describes the probability density of such estimates. The background is darker corresponding to many estimates with similar values and lighter when few estimates are present.

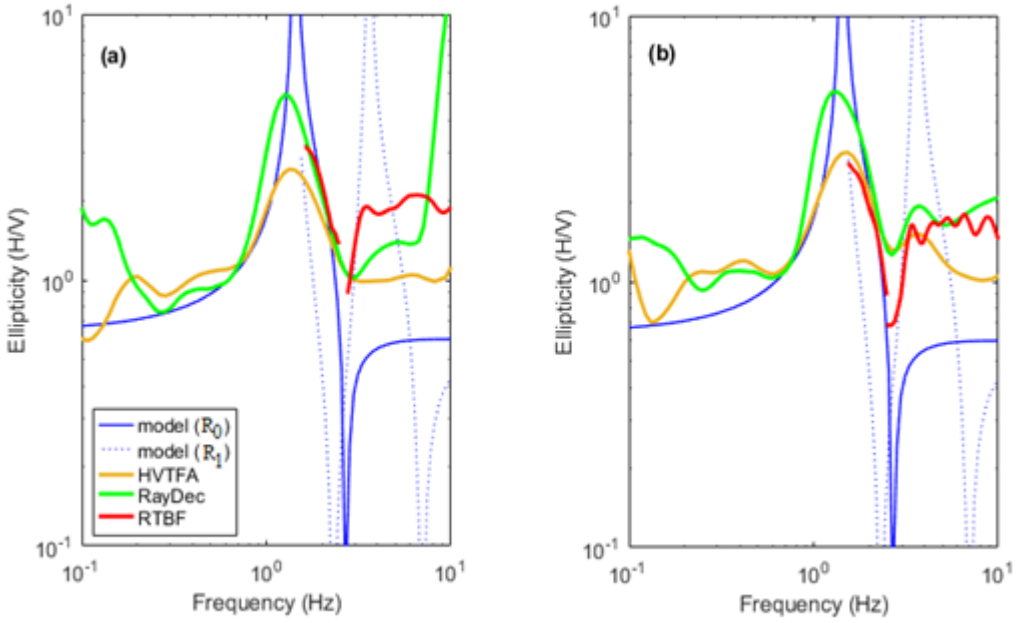

Fig 7. Ellipticity curves deduced from synthetic seismic noise data using HVTFA, RayDec and RTBF methods assuming (a) omnidirectional (b) non-omnidirectional distributions of noise sources. The ellipticity curves are compared to theoretical R_0 and R_1 curves which are displayed as solid and dotted blue curves, respectively.

cording to Fig. 6c, the picked ellipticity angle is fitted well to the theoretical model at right flank of peak frequency (from 1.5 to 2.7 Hz). Despite showing the same trend, the picked curve shows some differences at frequencies higher than 2.7 Hz, where the particle motion changed to retrograde. It is inferred that the different modes of Rayleigh and Love dispersion curves are better recognized assuming non-omnidirectional distribution of sources, while poor performances were found for omnidirectional distribution. It is probably due to the fact that the waves from different azimuths for omnidirectional distribution are present at the same time and then their amplitudes interfere.

3-2 Horizontal to vertical time frequency analysis (HVTFA)

Fäh et al. (2001, 2003) showed that the application of HVTFA can reduce the SH-wave influence by identifying P-SV wavelets from the signal and computing the spectral ratio from these wavelets. The vertical component is considered as a trigger and it is assumed that the most energetic wave arrivals correspond to Rayleigh waves. Later, Fäh et al. (2009) proposed to apply continuous wavelet transform (CWT) using the modified Morlet wavelet in time frequency analysis to detect pure Rayleigh waves. The horizontal signals are shifted by a quarter period of the given frequency, according to the characteristics of Rayleigh waves. Then for each identified maximum on vertical component, the corresponding maximum is searched for the horizontal component. The ratio of horizontal to vertical signals is stacked for each maximum.

The HVTFA method is applied on the central station of synthetic data to retrieve Rayleigh wave ellipticity curve. The results of two array data related to different distributions of noise source is compared with the theoretical model. As Fig. 7 shows, the method performs well in recognizing the peak frequency of the Rayleigh wave ellipticity curve for both distributions, while the right flank of

peak and trough frequencies are better estimated for non-omnidirectional case.

3-3 Rayleigh wave ellipticity estimation by Random Decrement technique (RayDec)

Hobiger et al. (2009) proposed a single station method, RayDec, to estimate ellipticity curve of Rayleigh wave based on the random decrement (RD) technique (Asmussen, 1997). The RD technique transforms a stochastic signal into a RD function based on some triggering conditions. Then, the vertical component is considered as a trigger and a large number of horizontal and vertical signals are stacked, which leads to emphasize Rayleigh waves and suppresses contributions of other wave types (Love and body waves) (Hobiger, 2011). The two horizontal components are then combined to a single horizontal component in a way to maximize the coherence with the vertical component, taking the quarter-period time shift between the vertical and horizontal components typical for Rayleigh waves into account. Next, the retrieved signals are stacked together and the ratio between the horizontal and vertical signals is estimated by analyzing the energy content of the vertical and horizontal stacks. It is repeated over the entire frequency range.

Here, the RayDec method is used to obtain Rayleigh wave ellipticity curve for central station of synthetic arrays. As discussed above, the theoretical fundamental peak and trough frequencies are at 1.5 and 2.7 Hz, respectively. According to Fig. 7, the peak frequency is a bit underestimated for both noise source distributions, whereas the right flank of peak frequency is better matched to the theoretical model in non-omnidirectional case.

In the following, the obtained ellipticity curves of HVTFA and RayDec and also ellipticity information retrieved by RTBF are compared for both distributions of noise sources (Fig. 7). In this regard, the resultant ellipticity angles deuced from RTBF are converted to ellipticity ratio by Eq. (1), and ellipticity angles are confined to array resolution limits. For omnidirectional distribution of noise sources (Fig. 7a), the HVTFA performs well to detect peak frequency at 1.5 Hz, while the amplitude and the right flank are better retrieved in RayDec. The RTBF shows poor performance to retrieve the ellipticity curve. In the case of non-omnidirectional distribution of noise sources, all considered methods show a good estimation of the right flank of peak frequency. The estimated peak frequency by HVTFA and RTBF are in good accordance with the theoretical one (Fig. 7b) and RayDec shows a better estimation of the amplitude of peak frequency. Furthermore, the trough frequency is better retrieved by RTBF.

Our findings revealed that the HVTFA and RayDec are less sensitive to the distributions of noise sources, while RTBF was found to be sensitive.

4 Methods and applications on real seismic noise measurements

The real seismic noise measured at a site in Ramsar (north of Iran) by Housing and Urban Development of Mazandaran in 2013 is used to study characteristics of surface waves. The data included six Nanometrics trillium 40 seismic stations which five stations placed on the circumference as well as a station at the center regarding array aperture of about 15 m. The length of the recording is 30 minutes with a sampling frequency of 100 Hz. The studied site is located near the Caspian Sea, which the distance is about 1600 m. The setup of receivers and locations of the array are shown in Fig. 8. Predominant stable directions of azimuth estimated using RTBF array method, lie in the range of 280 to 320 degrees clockwise from the North (Fig. 9a). This direction could be associated with the Caspian Sea (north-east of the array) as the origin of

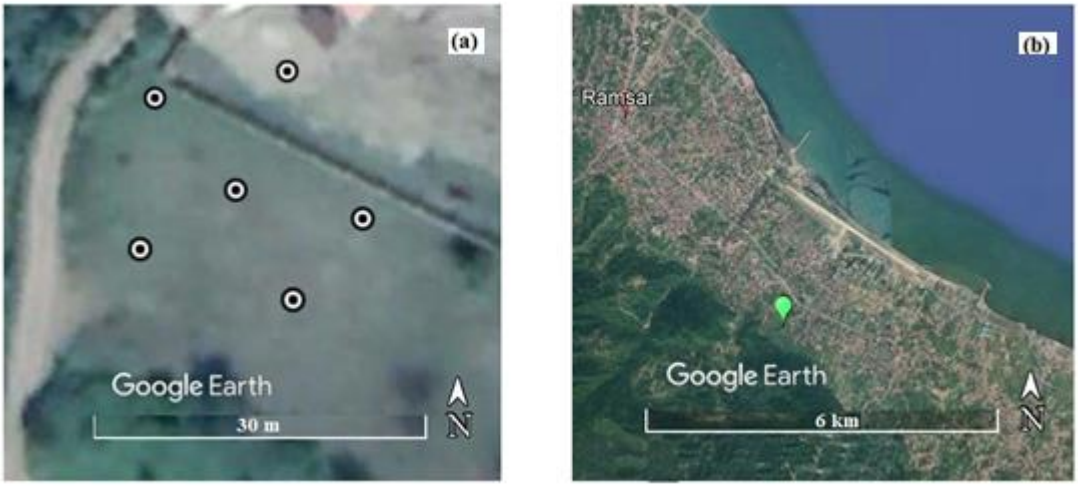

Fig 8. (a) The array layout of real seismic noise measurements in Ramsar (b) locations of the array which is depicted by green sign on the Google Earth map.

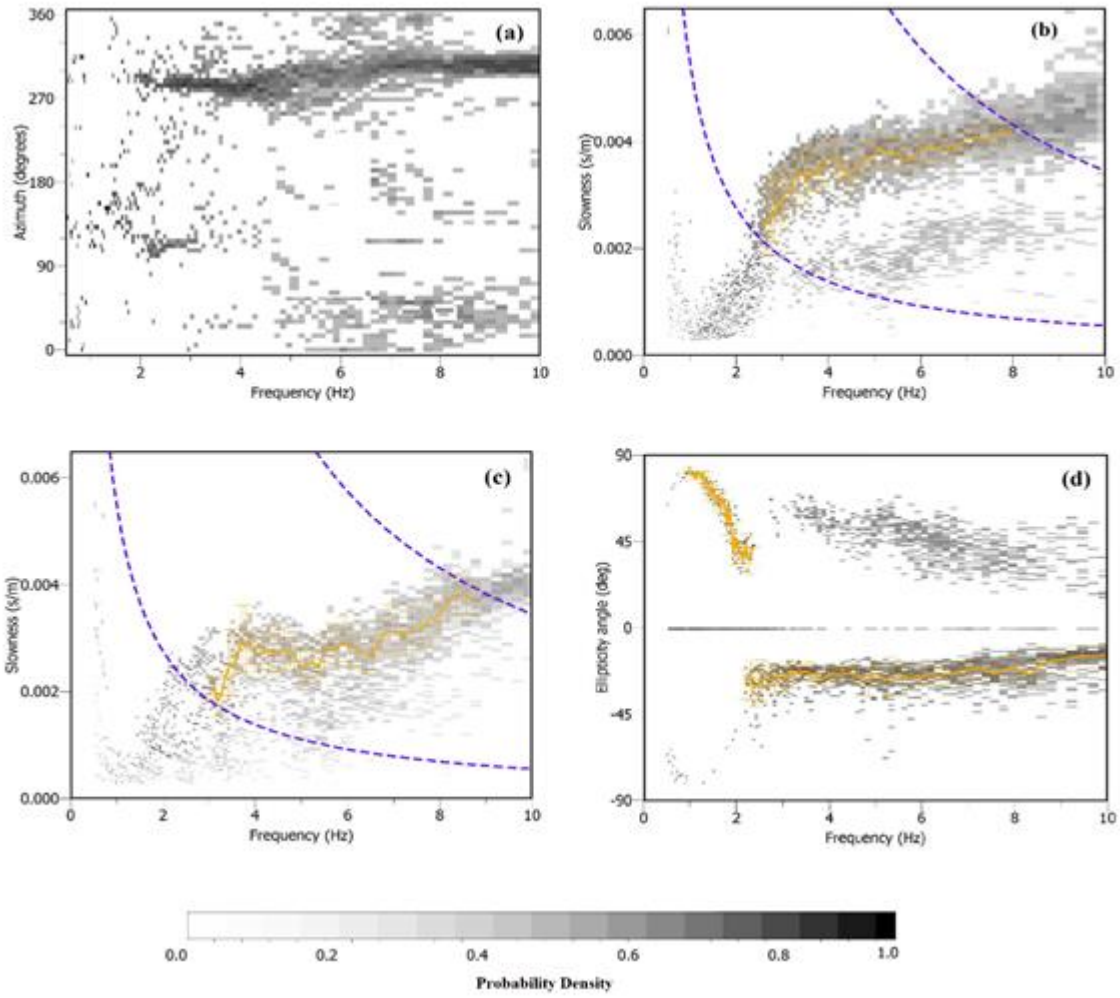

Fig 9. Applying RTBF method on Ramsar site (a) the estimated azimuth (b) the estimated Rayleigh wave dispersion curve and the picked R_0 (in orange color) (c) the estimated Love wave dispersion curve and the picked L_0 (in orange color) (d) the estimated Rayleigh wave ellipticity angle and the picked R_0 (in orange color). Besides, the array limits are shown by dashed blue curves.

the dominant seismic noise. Therefore, the site is studied as a typical case of non-omnidirectional distribution of noise sources around the array of stations.

As discussed above, the RTBF is applied on real seismic noise measurements in order to estimate Rayleigh and Love dispersion curves and ellipticity angle information. The trends of highest probability densities are picked as mean values and the resultant curves are depicted in orange color with the relevant error bars representing standard deviations. The picked R_0 and L_0 dispersion curves and the R_0 ellipticity angle are recognized in Figs. 9b-d. The ellipticity angle is prograde below 2.2 Hz, while it changes to retrograde for higher frequencies. However, the higher modes of dispersion and ellipticity curves were absent; they were not formed or recognizable by RTBF method. In order to compare the results of RTBF with HVTFA and RayDec methods, the resultant ellipticity angle of RTBF is converted to ellipticity curve by Eq. (1). As it is obvious in Fig. 10, the peak frequencies obtained from these methods are not completely accordant and slight differences are seen, whereas RTBF and RayDec detect similar trends for the right flank of the peak frequency. According to the results obtained from non-omnidirectional simulated distribution, retrieved right flank of peak frequency using RTBF or RayDec alongside the peak frequency obtained from HVTFA at 1.07 Hz could be acceptable to use in following process.

5 Shear wave velocity profile

We benefited the R_0 and L_0 dispersion curves and the right flank of the RTBF ellipticity curve alongside peak frequency determined by HVTFA to obtain the shear wave velocity of the studied site in Ramsar as a non-omnidirectional distribution case. We implemented the *Dinver* module of *Geopsy* (Wathelet et al., 2020), which is based on the modified conditional neighborhood algorithm (Wathelet, 2008).

The parameterization of the soil model achieved using a single layer as a stack of several sub-layers overlying a half space following a power law velocity with depth. The results are presented in Fig. 11. The minimum misfit value is about 0.1. The obtained shear wave velocity and the depth of bedrock at Ramsar site are about 2450 m/s and 94 m, respectively. As no acceptable geotechnical field studies has been fulfilled in the studied area, no information of the ground velocity profile was available to validate the

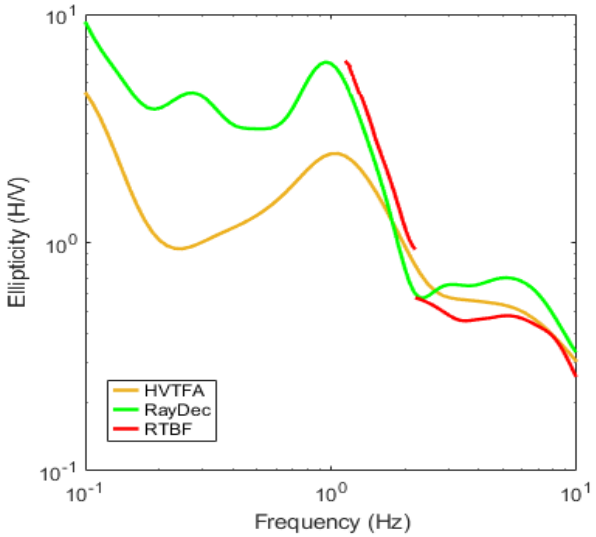

Fig 10. Ellipticity curves deduced from seismic ambient noise data recorded in Ramsar using HVTFA, RayDec and RTBF methods.

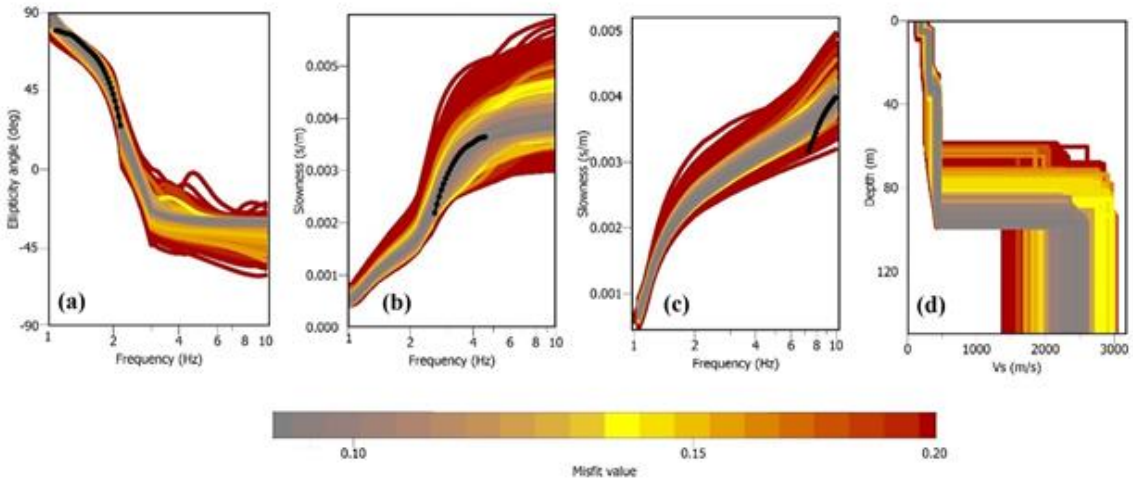

Fig 11. The Ramsar site (a) the observed R_0 ellipticity angle (the black dotted curve) (b) the observed R_0 dispersion curve (the black dotted curve) (c) the observed L_0 dispersion curve (the black dotted curve) (d) the estimated shear wave velocity model obtained from inversion.

results of the inversion. However, according to the geological studies of the area, shallow depth of bedrock is expected.

6 Discussion and conclusion

In this study, we investigated the dependency of surface wave characteristics on distributions of noise sources. Two datasets were simulated regarding the omnidirectional and non-omnidirectional distributions of noise sources around an array of six stations. The array signal processing technique RTBF alongside two well-known single station methods HVTFA and RayDec were applied to processing the synthetic noise data. The results of RTBF revealed good estimation of dispersion curves and the ellipticity angle in non-omnidirectional distribution. However, poor performances were found for omnidirectional distribution probably due to the fact that the waves from different azimuths are present at the same time and their amplitudes interfere. Our findings revealed that the HVTFA and RayDec are less sensitive to the distributions of noise sources, while RTBF was found to be sensitive.

Besides, the real seismic noise measured at a site in Ramsar (north of Iran) was processed to study surface wave properties regarding the non-omnidirectional predominated azimuthal distribution of noise sources. The dispersion and ellipticity curves were applied jointly to get shear wave velocity profile of subsoil structure beneath the studied site. The inversion results indicated the shear wave velocity and the depth of bedrock under the site were about 2450 m/s and 94 m, respectively. As the project of "Studies of Seismic Microzonation in Ramsar" was interrupted because of budget insufficiency, unfortunately no geotechnical evidences were available to justify the results of inversion. The proper comparisons will be added to the current study as the complementary information becomes available.

Data and Resources

The Geopsy software package, available at www.geopsy.org (last accessed November 2020).

Program FD designed for the finite-difference simulation of seismic wave propagation developed by Moczo and Kristek (2002) as a part of the SESAME project by European Commission- Research General Directorate. Project No. EVG1-CT-2000-00026 (available at http://SESAMEFP5.obs.ujf-grenoble.fr).

Acknowledgments

The authors thank the Housing and Urban Development Center of Mazandaran, for providing part of seismic noise data acquired by the Institute of Geophysics for the project of "Studies of Seismic Microzonation in Ramsar" which was applied in this research. Moreover, we appreciate the reviewers for their constructive comments which helped us to improve this manuscript.

References

Aki, K., 1957, Space and time spectra of stationary stochastic waves, with special reference to microtremors: Bulletin of the Earthquake Research Institute, **35**, 415-456.

Asmussen, J. C., 1997, Modal Analysis Based on the Random Decrement Technique: Application to Civil Engineering Structures: PhD thesis, University of Aalborg, Denmark.

Bonnefoy-Claudet, S., Cotton, F., and Bard, P. Y., 2006, The nature of noise wavefield and its applications for site effects studies, A literature review: Earth-Science Review, **79**, 205-227, doi 10.1016/j.earscirev.2006.07.004.

Capon, J., 1969, High-resolution frequency-wavenumber spectrum analysis: Proceeding of IEEE, **57**, 1408-1418, doi 10.1109/PROC.1969.7278.

Fäh, D., Kind, F., and Giardini, D., 2001, A theoretical investigation of average H/V ratios: Geophys. J. Int., **145**, 535-549.

Fäh, D., Kind, F., and Giardini, D., 2003, Inversion of local S-wave velocity structures from average H/V ratios, and their use for the estimation of site-effects: Journal of Seismology, **7**, 449-467, doi 10.1023/B:JOSE.0000005712.86058.42.

Fäh, D., Wathelet, M., Kristekova, M., Havenith, H., Endrun, B., Stamm, G., Poggi, V., Burjanek, J., and Cornou, C., 2009, Using Ellipticity Information for Site Characterisation: NERIES deliverable JRA4D4, Final Report, http://www.neries-jra4.geopsy.org.

Foti, S., Parolai, S., Albarello, D., and Picozzi, M., 2011, Application of Surface-Wave Methods for Seismic Site Characterization: Surveys Geophysics, **32**, 777–825. doi:10.1007/s10712-011-9134-2.

Hisada, Y., 1994, An efficient method for computing Green's functions for a layered half-space with sources and receivers at depths: Bull. Seism. Soc. Am., **84**(5), 1456-1472.

Hisada, Y., 1995, An efficient method for computing Green's functions for a layered half-space with sources and receivers at close depths (Part 2): Bull Seism. Soc. Am., **85**(4), 1080-1093.

Hobiger, M., Bard, P. Y., Cornou, C., and Le Bihan, N., 2009, Single station determination of Rayleigh wave ellipticity by using the random decrement technique (RayDec): Geophys. Res. Lett., 36, doi 10.1029/2009GL038863.

Hobiger, M., 2011, Polarization of surface waves: characterization, inversion and application to seismic hazard assessment: PhD thesis, University of Joseph Fourier, Grenoble, France.

Köhler, A., Ohrnberger, M., Scherbaum, F., Wathelet, M., and Cornou, C., 2007, Assessing the reliability of the modified three-component spatial autocorrelation technique: Geophys. J. Int., **168**, 779-796.

Lacoss, R. T., Kelly, E. J., and Toksöz, M. N., 1969, Estimation of seismic noise structure using arrays: Geophysics, **34**, 21-38, doi 10.1190/1.1439995.

Maranò, S., Reller, C., Loeliger, H. A., and Fäh, D., 2012, Seismic waves estimation and wavefield decomposition: Application to ambient vibrations: Geophys. J. Int., **191**, 175-188, doi:10.1111/j.1365-246X.2012.05593.x.

Moczo, P., and Kristek, J., 2002, FD Code to generate noise synthetics:

SESAME Rep. D02.09, IGSAS, Bratislava, http://SESAME-FP5.obs.ujf-grenoble.fr.

Nakamura, Y., 1989, A method for dynamic characteristics estimation of subsurface using microtremor on the ground surface: Quarterly Report of RTRI, **30**(1), 25-33.

Nogoshi, M., and Igarashi, T., 1971, On the amplitude characteristics of microtremor (Part 2): Journal of the Seismological Society of Japan, **24**, 26-40, https://doi.org/10.4294/zisin1948.24.1_26.

Poggi, V., and Fäh, D., 2010, Estimating Rayleigh wave particle motion from three-component array analysis of ambient vibrations: Geophys. J. Int., **180**, 251-267, doi 10.1111/j.1365-246X.2009.04402.x.

Wathelet, M., 2008, An improved neighborhood algorithm: parameter conditions and dynamic scaling: Geophys. Res. Lett., **35**, L09301, doi 10.1029/2008GL033256.

Wathelet, M., Guillier, B., Roux, P., Cornou, C., and Ohrnberger, M., 2018, Rayleigh wave three-component beamforming: Signed ellipticity assessment from high-resolution frequency-wavenumber processing of ambient vibration arrays: Geophys. J. Int., **215**(1), 507-523. Doi 10.1093/gji/ggy286.

Wathelet, M., Chatelain, J. L., Cornou, C., Giulio, G. D., Guillier, B., Ohrnberger, M., and Savvaidis, A., 2020, Geopsy: A user-friendly open-source tool set for ambient vibration processing: Seismol. Res. Lett., **91**(3), 1878-1889. doi:10.1785/0220190360.